Available online at www.sciencedirect.com
ScienceDirect
International Journal of Heat and Mass Transfer 51 (2008) 1205–1215
International Journal of HEAT and MASS TRANSFER
www.elsevier.com/locate/ijhmt

Heat transfer behavior in a rotating aluminum foam heat sink with a circular impinging jet

Tzer-Ming Jeng [a], Sheng-Chung Tzeng [b,*], Tung-Chun Liu [b]

[a] Department of Mechanical Engineering, Air Force Institute of Technology, GangShan 820, Taiwan, ROC
[b] Department of Mechanical Engineering, Chienkuo Technology University, ChanGhua 500, Taiwan, ROC

Received 8 September 2006; received in revised form 1 March 2007
Available online 2 May 2007

Abstract

This work experimentally studied heat transfer associated with an impinging jet onto a rotating heat sink. Air was used as the impinging coolant, and a square Al-foam heat sink was adopted. The variable parameters were the jet Reynolds number (Re), the relative nozzle-to-foam tip distance (C/d), the rotational Reynolds number (Re_r) and the relative side length of the square heat sink (L/d). The effects of Re, C/d, Re_r and L/d on the dimensionless temperature distributions and the average Nusselt number were considered. For a stationary system, the results reveal that the average Nusselt number (Nu_0) with Al-foam was two to three times that without Al-foam. Nu_0 increased with Re. A larger L/d responded to a larger Nu_0 based on the same jet flow rate. The effect of C/d on Nu_0 was negligible herein. For a rotating system, when Re and L/d were small and C/d was large, the average Nusselt number (Nu_Ω) increased considerably with Re_r. Additionally, for $Nu_\Omega/Nu_0 \geqslant 1.1$, the results suggest that rotation was substantial at $Re_r/Re \geqslant 1.13$ when $L/d = 4.615$ with $C/d =$ 0–5 and at $Re_r/Re \geqslant 1.07$ when $L/d = 3.0$ with $C/d = 0$–5. For $L/d = 2.222$, rotation was substantial at $Re_r/Re \geqslant 1.44$ when $C/d = 0$ and was always substantial when $C/d \geqslant 1$.

Keywords: Heat transfer; Jet impingement; Al-foam heat sink; Rotation

1. Introduction

The impinging of a jet onto a heated and stationary plate has attracted considerable interest since it can provide large localized heat transfer for many applications [1–10]. With respect to cooling following jet impingement, heat transfer is closely related to fluid flow. The characteristics of jet flow when the jet impinges orthogonally on a stationary plane surface have been investigated. Jambunathan et al. [1] reviewed the heat transfer data for a single circular jet impingement and summarized four flow zones that commonly are present in such systems. These are (1) the initial mixing zone, (2) the established jet zone, (3) the deflection zone and (4) the wall jet zone. Impinging cooling technology is used not only in the cooling of stationary systems, but also in rotating equipment, including rotational trays of chemical vapor deposition (CAD) systems, turbines and electric motors, rotating heat exchangers and high-speed gas bearings. Therefore, various investigations have been performed on the fluid flow and heat transfer characteristics of a rotating disk with an impinging jet [11–14]. The circumferential velocity component induced by rotation promotes convective heat transfer of the heated plate.

The heat sink with an extended surface is mounted on the heated plate to improve the cooling in an impinging jet system. As well as increasing the dissipation of the heat from the surface, the turbulence caused by the separation and reattachment of jet flow across the fins also facilitates the heat transfer between the flowing air and the fins. Related works are described below. Sathe et al. [15] presented a computational analysis of three-dimensional flow and heat transfer in the pin-fin heat sink. They reported

* Corresponding author. Tel.: +886 4 7111111x3182; fax: +886 4 7357193.
E-mail addresses: tsc@ctu.edu.tw, tsc33@ms32.hinet.net (S.-C. Tzeng).

0017-9310/$ - see front matter © 2007 Published by Elsevier Ltd.
doi:10.1016/j.ijheatmasstransfer.2007.03.011

Nomenclature

C	nozzle-to-foam tip distance (m)
d^*	inner diameter of the vertical tube connecting the nozzle (m)
d	inner diameter of the nozzle (m)
D^*	outer diameter of the nozzle (m)
D	diameter of the circular and heated plate (m)
h	heat transfer coefficient (W/m^2 °C)
H	nozzle-to-plate distance (m)
H_f	height of the al-foams (m)
k	conductivity (W/m °C)
L	side length of the square heat sink (m)
Nu	average Nusselt number, $Nu = \frac{hL}{k_f} = \frac{q_c L}{(\overline{T}_w - T_j)k_f}$
q_c	convective heat dissipated from the heated surface (W/m^2)
q_k	conductive heat loss (W/m^2)
q_r	radiative heat loss (W/m^2)
q_t	total heat flux (W/m^2)
Re	jet Reynolds number, $Re = \frac{\rho_f U_j d}{\mu}$
Re_r	rotational Reynolds number, $Re_r = \frac{\rho \pi \Omega L^2}{120\mu}$
t	thickness of the spreader (m)
T	temperature (°C)
U_j	average fluid velocity at the nozzle exit (m/s)
x	coordinate shown in Fig. 3 (m)

Greek symbols

ε	porosity of Al-foams
μ	viscosity of fluid (kg/m/s)
ρ	density (kg/m^3)
θ	nondimensional temperature, $\theta = \frac{T - T_j}{\overline{T}_w - T_j}$
Ω	rotational rate of the heat sink (rpm)

Subscripts

0	stationary state
f	fluid stream
w	heated wall
j	jet nozzle
Ω	rotational state

that the part of the heated base that was directly below the nozzle was effectively cooled and the temperature slowly increased from the center to the corner. Sparrow et al. [16–18] experimentally and theoretically studied the heat transfer from the in-line cylindrical pin-fins with an oncoming longitudinal flow which turned through 90° to exit the pin-fin array. They found that pin-fins situated next to the edges of the array had higher heat transfer coefficients than those situated inside the array. Additionally, they demonstrated that partial shrouding of the inlet could yield nearly uniform per-fin heat transfer coefficients throughout the array. Furthermore, changing the exit geometry influenced only the less tightly packed arrays and did so only at the outermost row of pin-fins. Hansen and Webb [19] experimentally investigated the heat transfer from the finned heat sink with a normally impinging air jet. The overall heat transfer in their systems was 1.5–4.5 greater than that in a bare plate. They also reported that heat transfer typically decreased as the nozzle diameter or H/d increased. Ledezma et al. [20] experimentally, numerically and theoretically examined the heat transfer from in-line square pin-fins with an oncoming longitudinal flow. They proposed optimized inter-fin spacing to maximize thermal conductance by varying the fin height, the fin thickness, the length of the side of the square base plate, the Prandtl number and the oncoming air velocity. Brignoni and Garimella [21] experimentally studied the heat transfer from the circular pin-fin heat sink with confined air jet impingement. They found that the nozzle-to-fin tip distance only slightly affected the heat transfer. The Nusselt number of the heat sink was 2.8–9.7 times that of a bare plate. Kondo et al. [22,23] proposed a zonal model, based on a series of semi-empirical formulae, to determine the thermal resistance and the pressure drop of the finned heat sinks with impingement cooling. They used the plate-fin heat sink and the circular pin-fin heat sink. Maveety et al. [24–26] experimentally and numerically investigated the heat transfer from the in-line square pin-fin heat sink with the impingement of a round air jet. They reported that performance was optimized when the relative nozzle-to-fin tip distance, C/d, was between 8 and 12 at $Re = 4 \times 10^4$–5×10^4. Moreover, using the approach of Ledezma et al. [20], they demonstrated that 7×7 pin-fin geometry outperformed 13×13 pin-fin geometry. Issa and Ortega [27] experimentally measured the pressure drop and heat transfer of a square jet that impinges onto a square pin-fin heat sink. Their concluded that the overall thermal resistance declined as the pin density or diameter increased. The effect of the pin-fin height on the thermal resistance was weak. Furthermore, short pin-fins at low Re were most strongly sensitive to variations in tip clearance. Lin et al. [28] experimentally studied the cooling performance of the plate-fin heat sinks with confined slot jet impingement. They proposed a complete composite correlation of steady-state average Nusselt number for mixed convection due to jet impingement and buoyancy.

Aluminum foams recently introduced as the heat sinks have large extended dissipation surface and added thermal dispersion conductivity to strongly promote cooling performance. Open cell structure of Aluminum foams is normally available with high porosities ($\varepsilon > 0.9$), resulting in a high permeability. The characteristic of the high permeability make Aluminum foam heat sinks very suitable for the jet impinging cooling scheme. Kim and his colleagues [29–31]

numerically and experimentally investigated the thermal performance of aluminum-foam and pin-fin heat sinks in a jet impingement. Their numerical results indicated that the anisotropy in permeability and effective thermal conductivity yields a significant change in the heat transfer rate. Besides, based on experimental data, they depicted that the multi-jet impingement shows higher heat transfer enhancement than the single jet impingement for high jet Reynolds number and smaller jet-to jet spacing. Shih et al. [32] experimentally explored the height effect on heat transfer of aluminum-foam cylinders with a circular jet impingement. The non-local thermal equilibrium regime was observed to exist at low Reynolds number and small dimensionless height.

The works herein improve our knowledge of the heat transferred by the impinging of a jet onto heat sinks. However, few experimental studies have addressed cooling by a jet that impinges on rotating heat sinks. This investigation elucidates the enhancement of heat transfer associated with jet impingement on a rotating heat sink. Air was used as an impinging coolant, and an Al-foam heat sink with 0.93 porosity (ε) and 10 PPI (pore per inch) was employed. Fig. 1a presents the aluminum foam sample, which has an open cell structure of aluminum fibers. Such a porous metallic material offers two advantages that promote heat transfer [33,34]: first, the porous material has a much larger dissipation area than does a conventional finned sink, increasing heat convection. Second, the irregular structure of the porous materials, at sufficiently large velocities, is responsible for the irregular motion of the fluid flow. The flow separates around the individual beads or fibers, mixing the fluid more effectively. Fig. 1b displays the physical model, whose variable parameters are the rate of flow, the diameter of the jet nozzle, the nozzle-to-foam tip distance and the rotational velocity. In such a system, the cooling performance of the heat sink is determine two forced convections – one from the jet impingement and the other associated with rotation. The local temperature distribution and average Nusselt number of such systems should be measured, to improve the cooling design of these systems.

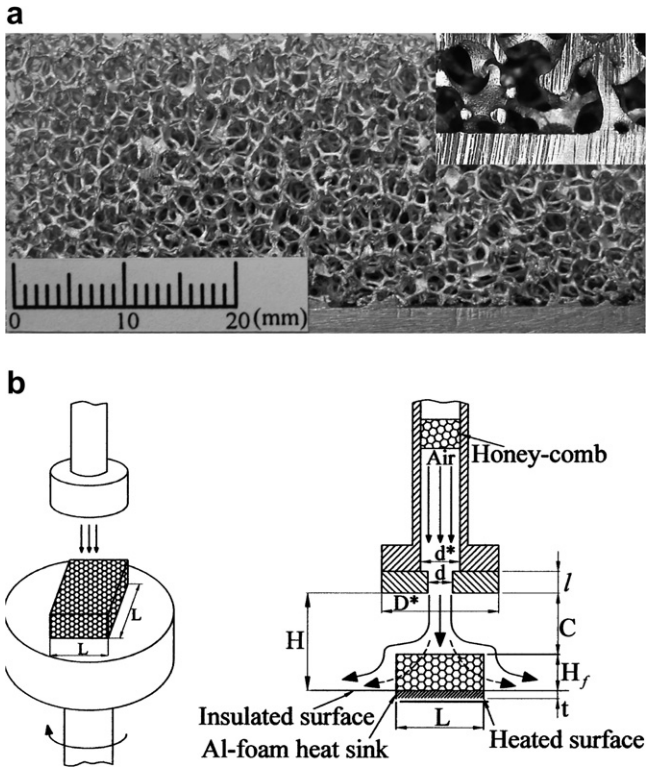

Fig. 1. Photograph of aluminum foam sample and physical model. (a) $\varepsilon = 0.93/10$PPI. (b) Physical model.

2. Experimental apparatus and test section

The experimental apparatus shown in Fig. 2 was designed to measure the heat transfer coefficient from the rotating heat sink to the jet air flow. The apparatus

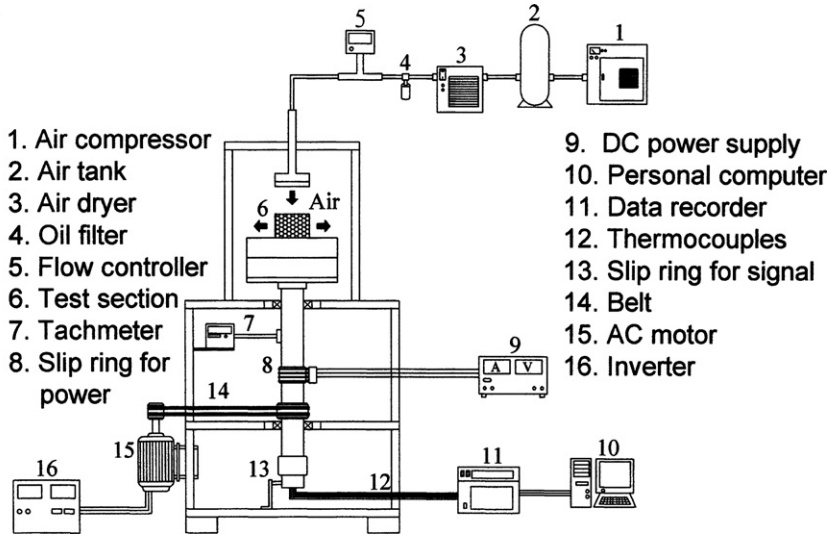

Fig. 2. Experimental apparatus.

consisted of four main parts: 1. rotating system; 2. test section; 3. data acquirement system, and 4. air supply system. The rotating system used a 5 HP AC induction motor that drove the rotating shaft via a belt pulley system. The rate of rotation was adjusted using an inverter to a maximum of 2000 rpm. Rates of rotation of 0, 600, 1000 and 1400 rpm were used. The rate of rotation was measured using a photo-electronic tachometer. The assembly of the rotating system and the test section was dynamically balanced. The test section was a rotary Bakelite disk with a diameter of 176 mm and a thickness of 50 mm. At the center of the Bakelite disk was a square 60 × 60 × 4 mm cavity. A film heater, which was heated using a dc power supply through a brush and a power slip ring, was attached to the square cavity. The input power to the heater was determined as the product of the voltage and the current, read using a precision shunt resistor. A 60 mm-length × 60 mm-width × 25.4 mm-height Al-foam block with 0.93 porosity (ε) and 10 PPI (pores per inch) was brazed onto 3.5 mm-thick aluminum spreader (as shown in the close-up view in Fig. 1a), and then attached to film heater using highly-conductive thermal grease (OMEGABOND 200, $k = 1.385$ W/m °C). The Bakelite disk has a very low conductivity and can reduce heat loss from the back of the film heater. Eight thermocouples were embedded in the cavity to measure the temperatures of the heat sink. Two were employed to measure the ambient temperature and the jet air temperature. They were connected to a YOKOGAWA 2500E data recorder through the data slip ring and the passage in the rotating shaft, which drove the rotation of the Bakelite disk. Fig. 3 presents the dimensions of the square Al-foam heat sink and the positions of the embedded TT-T-30SLE thermocouples. The jet air flow was blown into the air tank using the air compressor. The air initially flowed through a filter to remove the oil, the water and the particles, and then entered a 27 mm-diameter vertical pipe with a honey-comb section to straighten the fluid flow. It then passed through a circular nozzle, and finally impinged on the rotating heat sink. The circular nozzle had a length of 13 mm, an external diameter of 84.8 mm and three internal diameters of 13 mm, 20 mm and 27 mm. The jet air flow rates of 50, 100, 150, 200 and 250 l/min were used in the tests, as determined using a flow meter. The system was assumed to be in the steady state when the temperature varied by less than 0.2 °C in 15 min.

3. Data reduction and uncertainty analysis

The measured fluid velocities, the rates of rotation and the temperatures yielded the dimensionless wall temperatures (θ_w), the jet Reynolds numbers (Re), the rotational Reynolds number (Re_Ω) and the average Nusselt number (Nu), using

$$\theta_w = \frac{T_w - T_j}{\overline{T_w} - T_j} \tag{1}$$

$$Re = \frac{\rho_f U_j d}{\mu} \tag{2}$$

$$Re_r = \frac{\rho \pi \Omega L^2}{120\mu} \tag{3}$$

$$Nu = \frac{hL}{k_f} = \frac{q_c L}{(\overline{T_w} - T_j)k_f} \tag{4}$$

where T_w is the local temperature measured at the bottom skin of the Al-foam heat sink; $\overline{T_w}$ is the average temperature at the bottom skin of the Al-foam heat sink; T_j is the temperature of the air jet; q_c represents the convective heat flux; U_j is the average air velocity at the nozzle exit; d is the inner diameter of the jet nozzle; Ω is the rate of rotation of the Al-foam heat sink, and L is the side length of the square heat sink, respectively. The total heat flux (q_t) generated by the thermo-foil heater may be transformed into two heat transfer modes in the present experiment. These modes are, (1) the conductive heat loss, q_k, and (2)

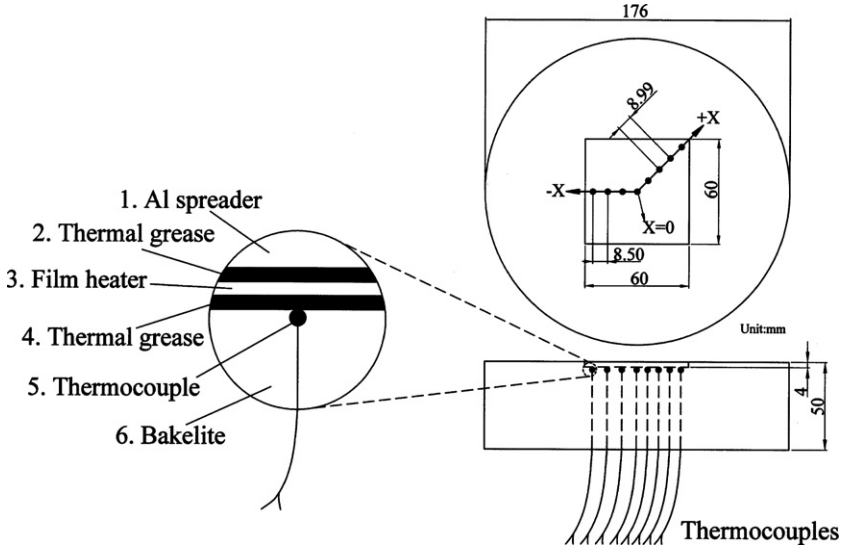

Fig. 3. Positions of thermocouples on the heated plate.

the convective heat dissipation, q_c, from the heated surface to the air jet flow, including the convective heat flux directly and indirectly (through solid (aluminum foam) phase by conduction) to the gas (air) phase. Therefore,

$$q_c = q_t - q_k \tag{5}$$

This energy-balance equation gives the net convective heat flux (q_c) from the heated surface to the jet air. The total heat flux (q_t) is V^2/R. Herein, V is the output voltage of the DC power supply and R is the resistance of the film heater. The conductive heat loss (q_k) to the insulated Bakelite is estimated using a two-dimensional conduction model. The q_k values vary from 3% to 29% of the total input heat flux throughout the experiments. Accordingly, the convective heat dissipated from the heated surface (q_c) can be determined and the average Nusselt number (Nu) is finally calculated.

The standard single-sample uncertainty analysis, as presented by Kline and McClintock [35] and Moffat [36], was performed. Data supplied by the manufacturer of the instruments stated that the flow velocity was measured with a 1% error. The uncertainty in the measured temperature was ±0.2 °C. The experimental uncertainty in the convective heat flux (q_c) was estimated to be 3.4%. The experimental data herein reveal that the uncertainties in the jet Reynolds number, the rotational Reynolds number, the dimensionless wall temperature and the average Nusselt number were 2.0%, 2.3%, 6.6% and 7.6% at 95% confidence, respectively.

4. Results and discussion

Fig. 4 displays the effects of Re, C/d, Re_r and L/d on the dimensionless temperature distributions along the x-axis. The results reveal that the dimensionless temperature (θ_w) distribution was fairly even, as θ_w was mostly between 0.95 and 1.05. Close observation reveals that when Re_r and C/d are large, the θ_w at the stagnation point ($x/L = 0$)

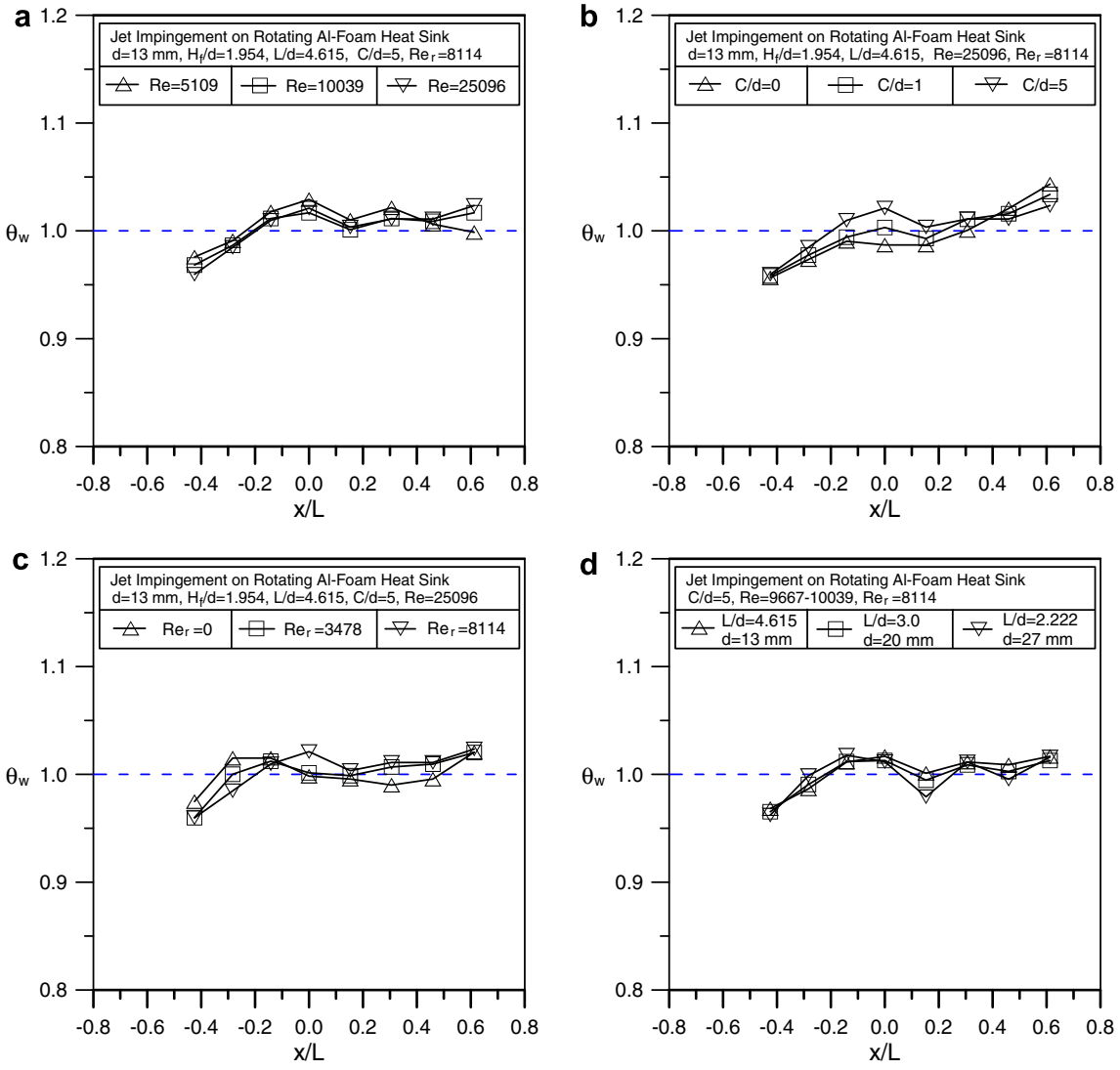

Fig. 4. Dimensionless temperature distributions for the typical cases. (a) Effect of Re; (b) effect of C/d; (c) effect of Re_r; (d) effect of L/d.

immediately below the nozzle exceeded the mean value one, indicating that the Nusselt number at that point was relatively small. The main reason is that the axial air velocities reduce with increasing distance from the nozzle exit which makes less air to go through the aluminum foams and reach the stagnation point, and the relative circumferential velocity by rotation of the aluminum foam heat sink will increase with increasing distance from the stagnation point. Additionally, at $x/L = -0.425$ (the side-edge of the heat sink shown in Fig. 3), θ_w was less than the mean value one. At $x/L = 0.613$ (the corner-edge of the heat sink presented in Fig. 3), θ_w exceeded the mean value one, because a shorter route has a smaller flow resistance. Therefore, more air flowed through the side-edge of the heat sink than the corner-edge of the heat sink.

Based on this discussion, Fig. 5 shows a sketch map of the flow pattern of this experimental system. The map does not show the angular velocity of rotation. A larger velocity vector indicates greater velocity. Theoretically, as more air flows into the aluminum foams and reaches the heated spreader, the effect of heat dissipation increases. The variables that influence the amount of air that enters the heat sink in the stationary system in this experiment are the velocity of jet flow, the nozzle-to-foam tip distance and the diameter of the nozzle. When rotation is considered, the air inside the aluminum foam heat sink generates relative circumferential velocity, promoting heat transfer. However, as the rotation of the heat sink promotes the transfer of heat, the rotating solid matrix blocks the

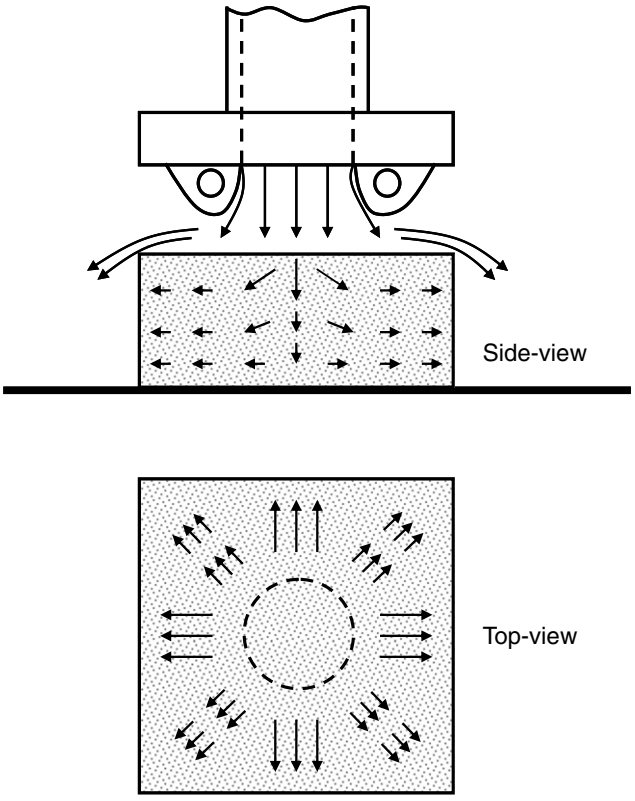

Fig. 5. Sketch map of flow pattern.

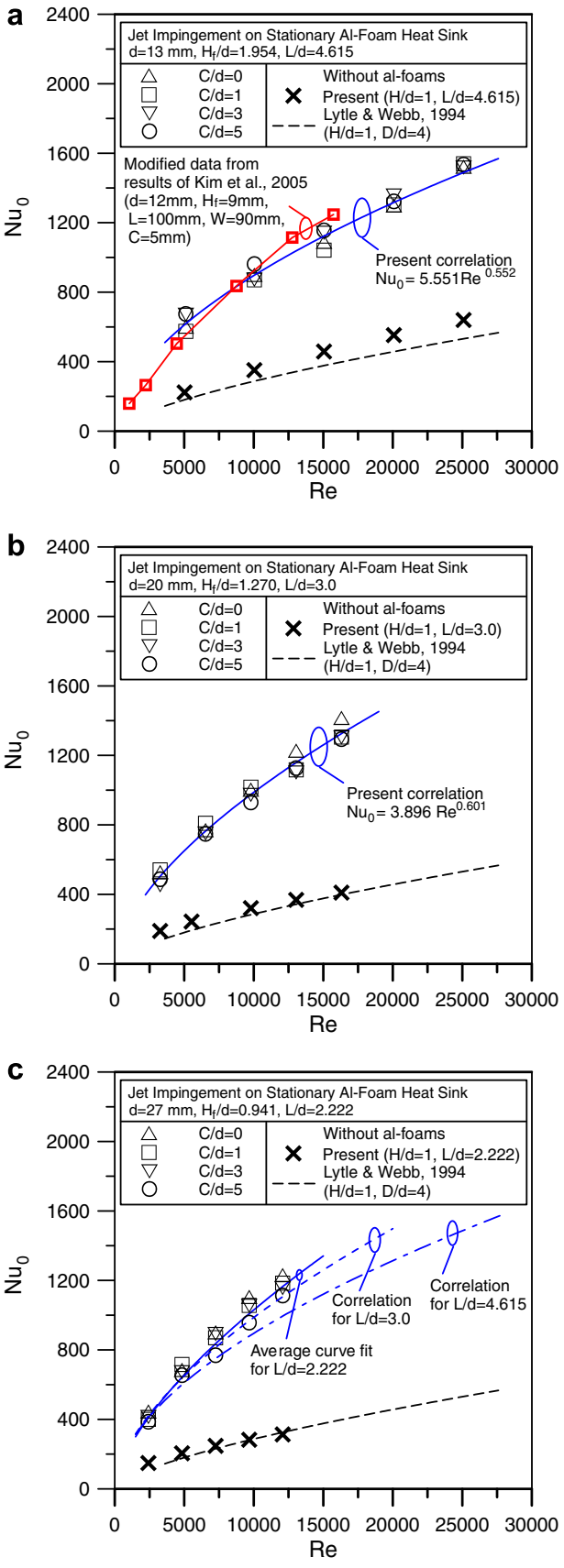

Fig. 6. Effect of jet Reynolds number on average Nusselt number of a stationary Aluminum foam heat sink with jet impingement (a) $L/d = 4.615$ (b) $L/d = 3.0$ (c) $L/d = 2.222$.

impinging jet, reducing the forced convection associated with jet impingement. The following section describes parametric studies of the effects of relevant parameters on heat transfer.

Fig. 6 plots the effects of Re, C/d and L/d on the average Nusselt number (Nu_0) of a stationary Al-foam heat sink with jet impingement. The results indicate that a larger jet Reynolds number corresponds to a larger average Nusselt number, characteristic of forced convection. The effect of C/d on the average Nusselt number was negligible when $L/d = 4.615$ or 3.0. The average Nusselt number seemed to slightly decrease with increasing C/d when $L/d = 2.222$. The main reason is that the jet air in the vicinity of outer perimeter of the jet nozzle easily bypass the aluminum foam heat sink at $L/d = 2.222$, especially under the condition that C/d is large. However, in the present study, the average Nusselt number only deviated from the average value within ±5% for systems with various C/d. Therefore, the effect of C/d on the average Nusselt number was negligible for the present system. In addition, as shown in Fig. 6c, reducing L/d slightly increases the average Nusselt number at a given Re. However, for the present definition of Reynolds number, the systems with the same Re but various L/d have different jet flow rates. There were five jet flow rates employed in the present experiments: 50, 100, 150, 200, 250 l/min. Based on the same jet flow rate, it is found that reducing L/d would decrease the average Nusselt number because the jet air in the vicinity of outer perimeter of the jet nozzle easily bypass the aluminum foam heat sink at small L/d.

Fig. 6 also plots the experimental data of Lytle and Webb [3] obtained using a system without heat sinks. The present heat transfer data of a stationary plate with jet impingement were reasonably consistent with those of

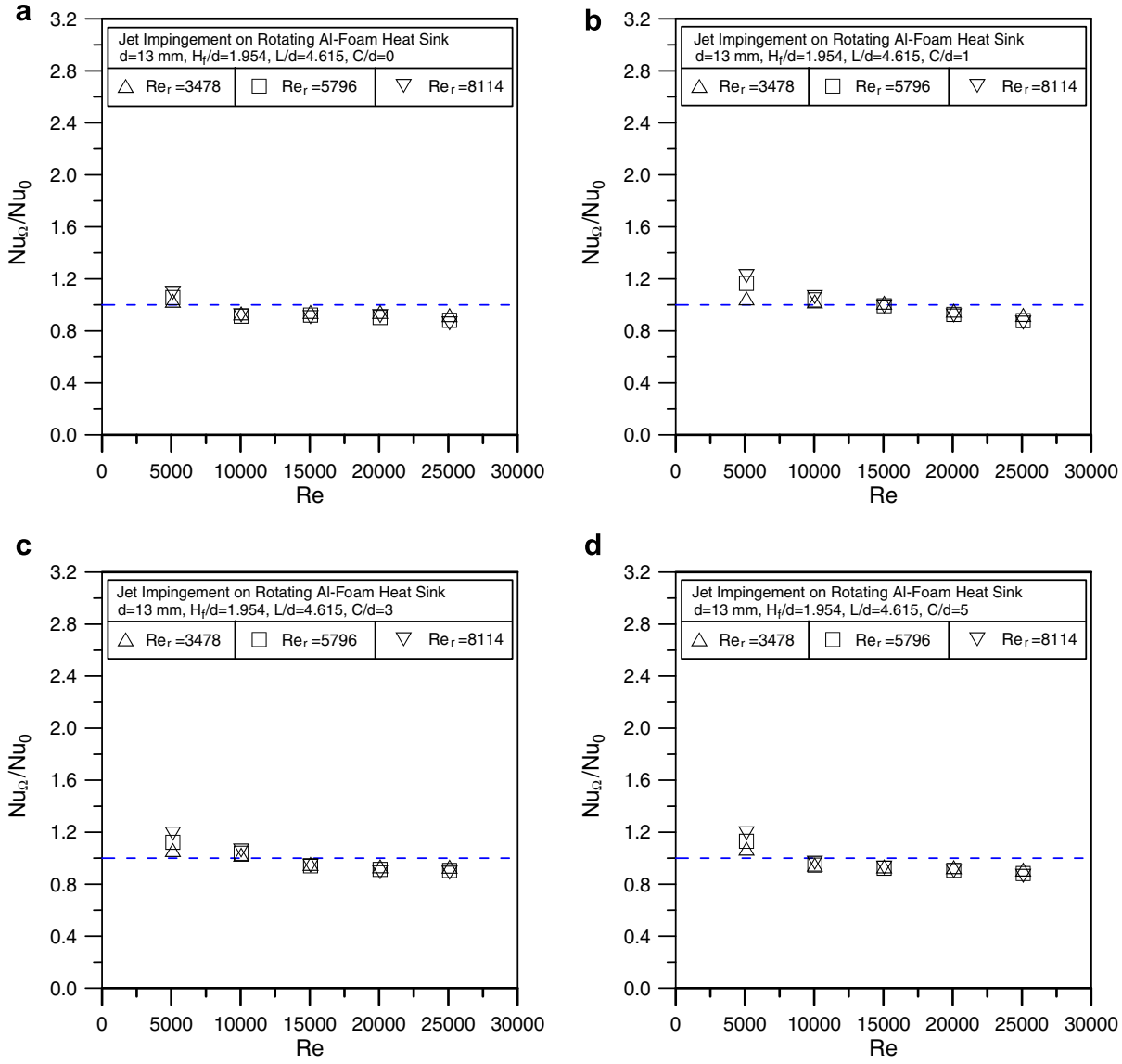

Fig. 7. Effect of rotational Reynolds number on average Nusselt number of a rotating aluminum foam heat sink with jet impingement ($L/d = 4.615$). (a) $C/d = 0$; (b) $C/d = 1$; (c) $C/d = 3$; (d) $C/d = 5$.

Lytle and Webb [3]. Comparing the heat transfer with/without Al-foams shows that the heat transfer through Al-foam was two to three times that without Al-foam. Kim et al. [31] also experimentally investigated the thermal performance of stationary aluminum-foam heat sinks in a multi-air jet impingement. One of their tests, single jet with $\varepsilon = 0.92/10$ PPI aluminum foam heat sink which was similar with the present stationary system, was used to be the compared case. Because the sizes of their aluminum foams (100 mm-length × 90 mm-width × 9 mm-height) and heated surface (100 mm-length × 90 mm-width) were different from those of the present system, for a fair comparison with cooling performance, their data of heat transfer coefficients were modified by multiplying the volume ratio of the present Al-foams to their one and the area ratio of their heated surface to the present one. The comparison result shown in Fig. 6a depicts that the modified data of Kim et al. [31] were reasonably consistent with the present results. The experimental data in Fig. 6 yield the following relationships between the average Nusselt number and the jet Reynolds number for a stationary Al-foam heat sink with various L/d and C/d values.

$$Nu_0 = 1.121(L/d)^{1.076} \times Re^{0.777(L/d)^{-0.227}} \quad \text{for} \quad L/d = 2.222\text{–}4.615 \quad \text{and} \quad C/d = 0\text{–}5 \tag{6}$$

The deviations between the predictions of Eq. (6) and the experimental data are within 5.39%.

Figs. 7–9 separately depict cases with $L/d = 4.615$, $L/d = 3.0$ and $L/d = 2.222$, and present the effect of rotational Reynolds number (Re_r) on average Nusselt number (Nu_Ω) of a rotating Al-foam heat sink with jet impingements for various Re and C/d. The relationship between Nu_Ω/Nu_0 and Re was plotted. The results demonstrate that a bigger Re_r meant a more obvious heat transfer enhancement in the case of smaller Re, but the heat transfer

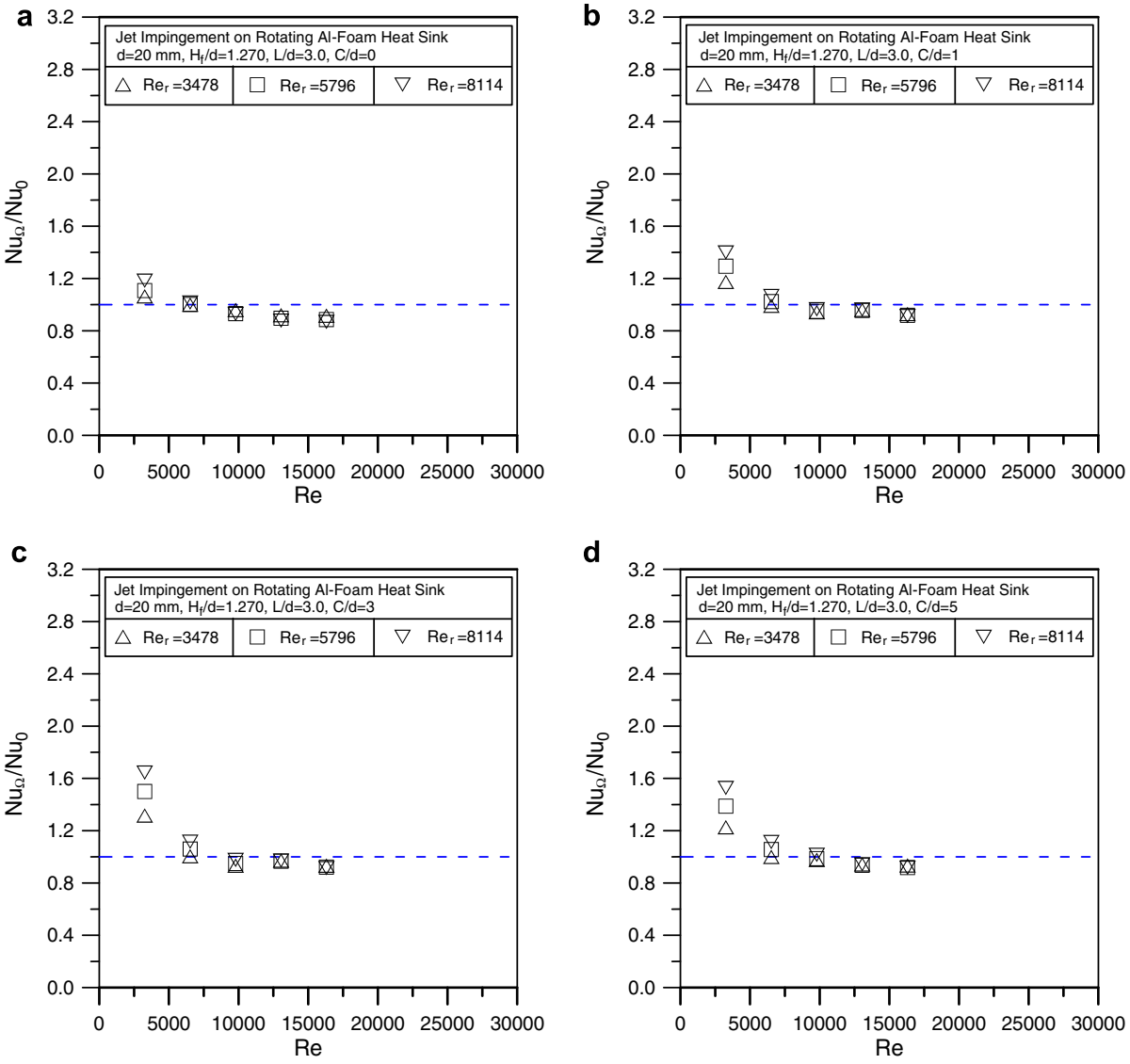

Fig. 8. Effect of rotational Reynolds number on average Nusselt number of a rotating aluminum foam heat sink with jet impingement ($L/d = 3.0$). (a) $C/d = 0$; (b) $C/d = 1$; (c) $C/d = 3$; (d) $C/d = 5$.

enhancement by rotation decreased with increasing Re. For the systems with ($L/d = 4.615$, $C/d = 0$–5), ($L/d = 3.0$, $C/d = 0$–5) and ($L/d = 2.222$, $C/d = 0$), the rotation even impaired the heat transfer at $Re > 10039$, $Re > 6525$ and $Re > 4833$, respectively. The reason can be explained as follows. When the aluminum foam heat sink is rotating, the inside air generates the peripheral velocity related to the solid matrix, promoting heat transfer. On the other hand, the rotating aluminum foams stops the jet flow from going through the solid matrix and reaching the heated spreader, reducing the heat transfer by the jet impingement. Therefore, if the heat transfer enhancement by rotation cannot compensate for the heat transfer reduction by rotation, the average Nusselt number at rotational state will less than that at stationary state (i.e. $Nu_\Omega/Nu_0 < 1$). At $L/d = 2.222$ with $C/d = 1$–5, the enhancement of heat transfer by rotation was marked for all Re. When L/d was small and C/d was large, the jet air in the vicinity of outer perimeter of the jet nozzle easily bypasses the aluminum foam heat sink. Less air inside aluminum foams results less impaired effect on impinging cooling performance by rotation. Besides, the rotation also perturbed the by-pass air flow around the heat sink to promote the heat transfer. So the average Nusselt number at rotational state was generally higher than that at stationary state (i.e. $Nu_\Omega/Nu_0 > 1$) at the system with small L/d and large C/d.

In principle, heat transfer enhancement increases with Re_r. However, the heat transfer varied little with Re increases, possibly because two forced convections apply – one associated with jet impingement, and the other associated with rotation. When Re is sufficiently large in relation to Re_r, the forced convection associated with jet impingement dominates the cooling performance and that associated with rotation is negligible. Therefore, a dimensionless parameter, Re_r/Re, can be utilized to identify whether the rotation is substantial. Fig. 10 plots Nu_Ω/Nu_0 as a function of Re_r/Re. Considering the experimental uncertainty yielded a value of Nu_Ω/Nu_0 of larger than 1.1

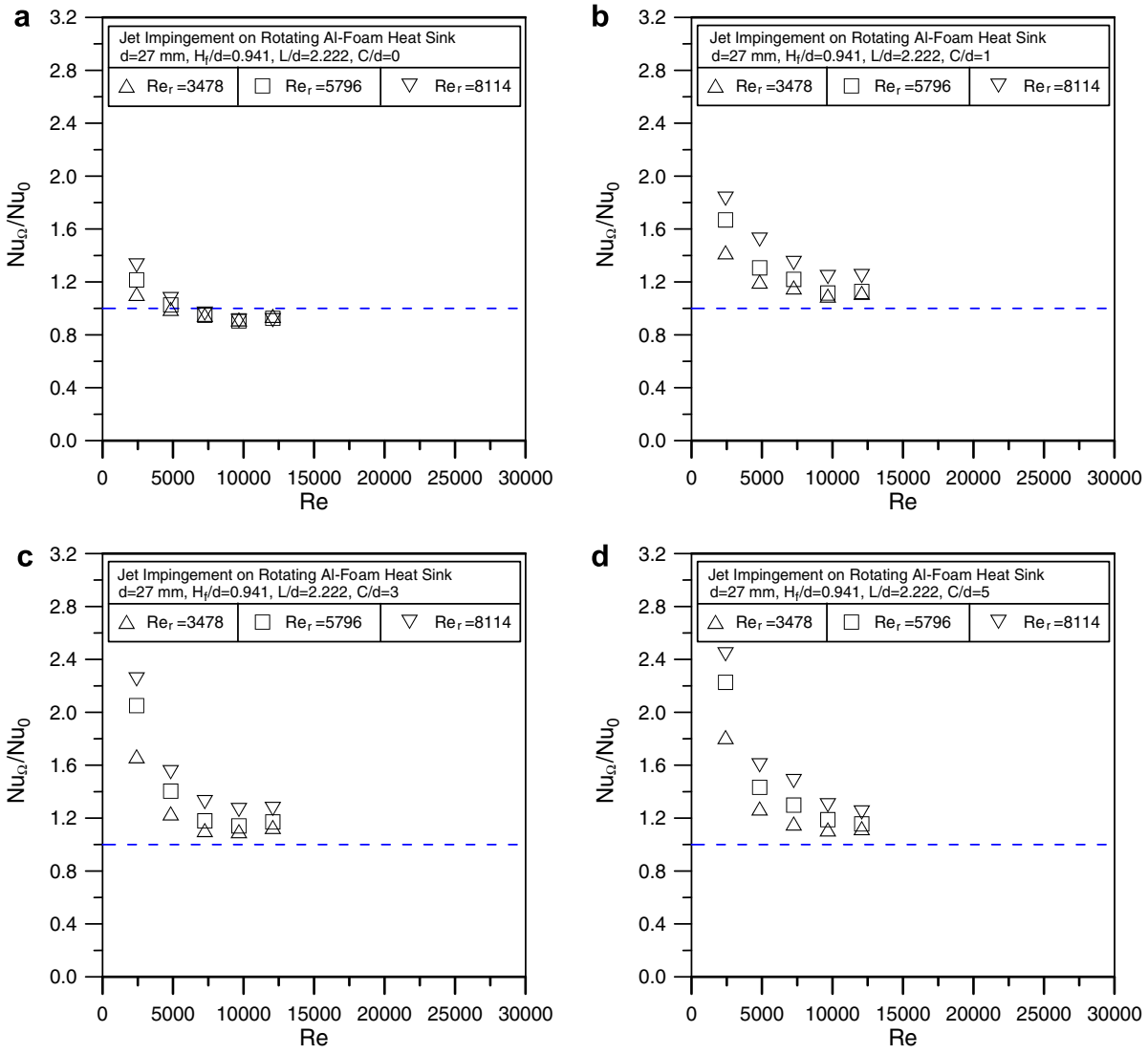

Fig. 9. Effect of rotational Reynolds number on average Nusselt number of a rotating aluminum foam heat sink with jet impingement ($L/d = 2.222$). (a) $C/d = 0$; (b) $C/d = 1$; (c) $C/d = 3$; (d) $C/d = 5$.

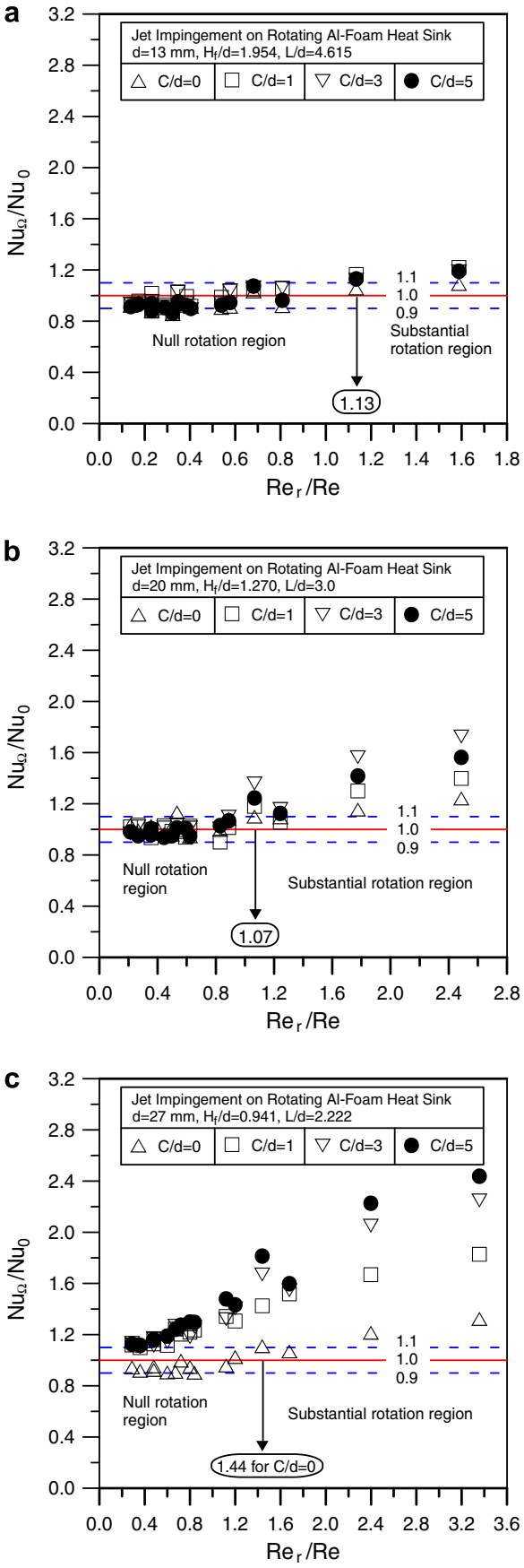

Fig. 10. Nu_Ω/Nu_0 as a function of Re_r/Re. (a) $L/d = 4.615$; (b) $L/d = 3.0$; (c) $L/d = 2.222$.

as the effective enhancement factor of heat transfer. Given $Nu_\Omega/Nu_0 \geqslant 1.1$, the results indicate substantial rotations at $Re_r/Re \geqslant 1.13$ and $Re_r/Re \geqslant 1.07$ for $L/d = 4.615$ with $C/d = 0$–5 and $L/d = 3.0$ with $C/d = 0$–5, respectively. For $L/d = 2.222$ with $C/d = 0$–5, rotation was substantial at $Re_r/Re \geqslant 1.44$ for $C/d = 0$; the rotation was always substantial for $C/d \geqslant 1$.

5. Summary and conclusion

Heat transfer associated with jet impingement on rotating porous heats sink was experimentally investigated. Air was used as an impinging coolant and a square Al-foam heat sink with $\varepsilon = 0.93$/10PPI was adopted. The variable parameters were the jet Reynolds number (Re), the relative nozzle-to-foam tip distance (C/d), the rotational Reynolds number (Re_r) and the relative side length of the square heat sink (L/d). The following conclusions are drawn.

(1) The effects of Re, C/d, Re_r and L/d on the dimensionless temperature distributions along the x-axis were presented. Experimental results reveal that the dimensionless temperature (θ_w) distribution was fairly even, as θ_w was mostly between 0.95 and 1.05. Close observation indicates that θ_w was less than the mean value one at the side-edge of the heat sink and exceeded the mean value one at the corner-edge of the heat sink.

(2) The effects of Re, C/d and L/d on the average Nusselt number (Nu_0) of a stationary Al-foam heat sink with jet impingement were presented. The Nu_0 obtained using Al-foams was two to three times that obtained without Al-foams. A larger Re corresponds to a larger Nu_0. Additionally, the effect of C/d on Nu_0 was insignificant herein. A larger L/d is associated with a slightly larger Nu_0 based on the same jet flow rate. Finally, the relationship between Nu_0 and Re for a stationary Al-foam heat sink with $L/d = 2.222$–4.615 and $C/d = 0$–5 was elucidated.

(3) The average Nusselt number (Nu_Ω) associated with rotating Al-foam heat sinks under an impinging jet for various Re, C/d, Re_r and L/d was presented. The results reveal that when Re and L/d were small and C/d was large, Re_r significantly promoted Nu_Ω. Additionally, according to $Nu_\Omega/Nu_0 \geqslant 1.1$, the results indicate that rotation was substantial at $Re_r/Re \geqslant 1.13$ and $Re_r/Re \geqslant 1.07$ for $L/d = 4.615$ with $C/d = 0$–5 and for $L/d = 3.0$ with $C/d = 0$–5, respectively. For $L/d = 2.222$ with $C/d = 0$–5, the rotation was substantial at $Re_r/Re \geqslant 1.44$ for $C/d = 0$; the rotation was always substantial for $C/d \geqslant 1$.

References

[1] K. Jambunathan, E. Lai, M.A. Moss, B.L. Button, A review of heat transfer data for single circular jet impingement, Int. J. Heat Fluid Flow 13 (2) (1992) 106–115.

[2] D.J. Womac, S. Ramadhyani, F.P. Incropera, Correlating equations for impingement cooling of small heat sources with single circular liquid jets, J. Heat Transfer 115 (1993) 106–115.
[3] D. Lytle, B.W. Webb, Air jet impingement heat transfer at low nozzle-plate spacings, Int. J. Heat Mass Transfer 37 (12) (1994) 1687–1697.
[4] J.Y. San, C.H. Huang, M.H. Shu, Impingement cooling of a confined circular air jet, Int. J. Heat Mass Transfer 40 (6) (1997) 1355–1364.
[5] M. Behnia, S. Parneix, Y. Shabany, P.A. Durbin, Numerical study of turbulent heat transfer in confined and unconfined impinging jets, Int. J. Heat Fluid Flow 20 (1999) 1–9.
[6] A.H. Beitelmal, M.A. Saad, C.D. Patel, Effects of surface roughness on the average heat transfer of an impinging air jet, Int. Commun. Heat Mass Transfer 27 (1) (2000) 1–12.
[7] H. Fujimoto, H. Takuda, N. Hatta, R. Viskanta, Numerical simulation of transient cooling of a hot solid by an impinging free surface jet, Numer. Heat Transfer Part A 36 (1999) 767–780.
[8] A.J. Bula, M.M. Rahman, J.E. Leland, Numerical modeling of conjugate heat transfer during impingement of free liquid jet issuing from a slot nozzle, Numer. Heat Transfer Part A 38 (2000) 45–66.
[9] D. Sahoo, M.A.R. Sharif, Mixed-convective cooling of an isothermal hot surface by confined slot jet impingement, Numer. Heat Transfer Part A 45 (2004) 887–909.
[10] M.K. Jeddi, S.K. Hannani, B. Farhanieh, Study of mixed-convection heat transfer from an impinging jet to a solid wall using a finite-element method – application to cook top modeling, Numer. Heat Transfer Part A 46 (2004) 387–397.
[11] M. Itoh, M. Okada, An experimental study of the radial wall jet on a rotating disk, Exper. Therm. Fluid Sci. 17 (1998) 49–56.
[12] Y.R. Shieh, C.J. Li, Y.H. Hung, Heat transfer from a horizontal wafer-based disk of multi-chip modules, Int. J. Heat Mass Transfer 42 (1999) 1007–1022.
[13] M.M. Rahman, Analysis of simultaneous gas absorption and chemical reaction to a thin liquid film over a spinning disk, Int. Commun. Heat Mass Transfer 27 (2000) 303–314.
[14] Y. Minagawa, S. Obi, Development of turbulent impinging jet on a rotating disk, Int. J. Heat Fluid Flow 25 (2004) 759–766.
[15] S. Sathe, K.M. Kelkar, K.C. Karki, C. Lamb, S.V. Patankar, Numerical predication of flow and heat transfer in an impingement heat sink, ASME J. Electron. Packag. 119 (1997) 58–63.
[16] E.M. Sparrow, E.D. Larson, Heat transfer from pin-fins situated in an oncoming longitudinal flow which turns to crossflow, Int. J. Heat Mass Transfer 25 (5) (1982) 603–613.
[17] E.D. Larson, E.M. Sparrow, Performance comparisons among geometrically different pin-fin arrays situated in an oncoming longitudinal flow, Int. J. Heat Mass Transfer 25 (5) (1982) 723–725.
[18] E.M. Sparrow, A.P. Suopys, M.A. Ansari, Effect of inlet, exit, and fin geometry on pin fins situated in a turning flow, Int. J. Heat Mass Transfer 27 (7) (1984) 1039–1054.
[19] L.G. Hansen, B.W. Webb, Air jet impingement heat transfer from modified surfaces, Int. J. Heat Mass Transfer 36 (4) (1993) 989–997.
[20] G. Ledezma, A.M. Morega, A. Bejan, Optimal spacing between pin fins with impinging flow, ASME J. Heat Transfer 118 (1996) 570–577.
[21] L.A. Brignoni, S.V. Garimella, Experimental optimization of confined air jet impingement on a pin fin heat sink, IEEE Trans. Comp. Packag. Technol. 22 (3) (1999) 399–404.
[22] Y. Kondo, M. Behnia, W. Nakayama, H. Matsushima, Optimization of finned heat sinks for impingement cooling of electronic packages, ASME J. Electron. Packag. 120 (1998) 259–266.
[23] Y. Kondo, H. Matsushima, T. Komatsu, Optimization of pin-fin heat sinks for impingement cooling of electronic packages, ASME J. Electron. Packag. 122 (2000) 240–246.
[24] J.G. Maveety, J.F. Hendricks, A heat sink performance study considering material, geometry, nozzle placement, and Reynolds number with air impingement, ASME J. Electron. Packag. 121 (1999) 156–161.
[25] J.G. Maveety, H.H. Jung, Design of an optimal pin-fin heat sink with air impingement cooling, Int. Commun. Heat Mass Transfer 27 (2) (2000) 229–239.
[26] J.G. Maveety, H.H. Jung, Heat transfer from square pin-fin heat sinks using air impingement cooling, IEEE Trans. Comp. Packag. Technol. 25 (3) (2002) 459–469.
[27] J.S. Issa, A. Ortega, Experimental measurements of the flow and heat transfer of a square jet impinging on an array of square pin fins, ASME J. Electron. Packag. 128 (2006) 61–70.
[28] T.W. Lin, M.C. Wu, L.K. Liu, C.J. Fang, Y.H. Hung, Cooling performance of using a confined slot jet impinging onto heated heat sinks, ASME J. Electron. Packag. 128 (2006) 82–91.
[29] S.Y. Kim, J.M. Koo, A.V. Kuznetsov, Effect of anisotropy in permeability and effective thermal conductivity on thermal performance of an aluminum foam heat sink, Numer. Heat Transfer Part A 40 (2001) 21–36.
[30] S.Y. Kim, A.V. Kuznetsov, Optimization of pin-fin heat sinks using anisotropic local thermal nonequilibrium porous model in a jet impinging channel, Numer. Heat Transfer Part A 44 (2003) 771–787.
[31] S.Y. Kim, M.H. Lee, K.S. Lee, Heat removal by aluminum-foam heat sinks in a multi-air jet impingement, IEEE Trans. Comp. Packag. Technol. 28 (2005) 142–148.
[32] W.H. Shih, W.C. Chiu, W.H. Hsieh, Height effect on heat-transfer characteristics of aluminum-foam heat sinks, ASME J. Heat Transfer 128 (2006) 530–537.
[33] V.V. Calmidi, R.L. Mahajan, Forced convection in high porosity metal foams, ASME J. Heat Transfer 122 (2000) 557–565.
[34] S.C. Tzeng, T.M. Jeng, Convective heat transfer in porous channels with 90-deg turned flow, Int. J. Heat Mass Transfer 49 (2006) 1452–1461.
[35] S.J. Kline, F.A. Mcclintock, Describing uncertainties in single-sample experiments, Mech. Eng. (1953) 3–8.
[36] R.J. Moffat, Contributions to the theory of single-sample uncertainty analysis, ASME J. Fluids Eng. 104 (1986) 250–260.